Structure and superconductivity in alkali-ammonia complex fullerides

Iwasa, Y.; Shimoda, H.; Miyamoto, Y.; Mitani, T.; Maniwa, Y.; Zhou, O.; Palstra, T.T.M.

Published in:
Journal of Physics and Chemistry of Solids

DOI:
10.1016/S0022-3697(97)00054-1

Publication date:
1997

Pergamon

PII: S0022-3697(97)00054-1

J. Phys. Chem Solids Vol 58, No. 11, pp. 1697–1705, 1997

0022-3697/97 $17.00 + 0.00

STRUCTURE AND SUPERCONDUCTIVITY IN ALKALI–AMMONIA COMPLEX FULLERIDES

Y. IWASA, H. SHIMODA, Y. MIYAMOTO, T. MITANI, Y. MANIWA[a], O. ZHOU[b,*] and T.T.M. PALSTRA[c,†]

Japan Advanced Institute of Science and Technology, Tatsunokuchi, Ishikawa 923-12, Japan
[a]Department of Physics, Tokyo Metroplitan University, Minami-osawa, Hachioji, Tokyo 192-03, Japan
[b]Fundamental Research Laboratories, NEC Corporation, 34 Miyukigaoka, Tsukuba 305, Japan
[c]AT&T Bell Laboratories, 600 Mountain Avenue, Murray Hill, New Jersey 07974, USA

Abstract—Alkali ammonia complex fullerides form a rich variety of compounds with unique structural and electronic properties. Intercalation of NH_3 into K_3C_{60} produces orthorhombic NH_3C_{60}, which undergoes a metal–insulator transition instead of superconductivity that is expected to occur at around 30 K from the empirical relation between T_c and the lattice parameter. Synthesis in liquid ammonia yields new superconducting fullerides $(NH_3)_xNaA_2C_{60}$ ($0.5 < x < 1$, A = K, Rb). While these compounds retain an fcc cell, they exhibit anomalous dependence of T_c on the lattice. These two examples suggest that the off-centred cations in the octahedral site have a serious effect on superconductivity. © 1997 Elsevier Science Ltd.

1. INTRODUCTION

T_c of superconductivity in fcc fullerides is controlled by the lattice parameter [1, 2]. The increase of T_c with lattice parameters suggests that the superconductivity of fullerenes falls in the framework of a weak coupling BCS mechanism [3]. This simple empirical rule has motivated many efforts in the synthesis of high-T_c fullerides with large lattice parameters. Intercalation of NH_3, which is the main subject of this paper, is one of the most successful means to expand the lattice parameters [4].

Another interesting property of fullerides is that the superconductivity is not seriously affected by several kinds of disorder, such as orientational disorder of C_{60} molecules and substitutional disorder of the interstitials sites in the binary intercalated systems. The tolerance for disorders is in sharp contrast with other molecular superconductors, such as BEDT–TTF-based materials [5]. Here, BEDT–TTF denotes bis(ethylenedithio)tetrathiafulvalene. Ammoniation of alkali C_{60} compounds introduces new types of disorder, such as rotation of ammonia molecules and positional disorders of ammonia molecules or cations. The effect of such disorders on superconductivity is an interesting issue in alkali ammonia complex systems.

The most successful results are obtained by ammoniation of Na_2CsC_{60} [4]. Exposing preformed Na_2CsC_{60} to NH_3 gas, followed by a 100°C anneal, yields fcc $(NH_3)_4Na_2CsC_{60}$ which shows a cell expansion from $a = 14.132$ Å to $a = 14.47$ Å, and an almost tripled T_c of 29.7 K. In this case, neutral NH_3 molecules are intercalated as spacers and successfully increased the cell dimension without symmetry lowering.

In other cases, intercalation of NH_3 causes structural distortion from fcc [6]. Reaction of K_3C_{60} with NH_3 produced $NH_3K_3C_{60}$, which has an orthorhombic structure of $a = 14.971$ Å, $b = 14.895$ Å, $c = 13.687$ Å. In this compound, each octahedral K is coordinated to one NH_3 molecule and is displaced away from the centre of the octahedral site. The unit cell volume of the $NH_3K_3C_{60}$ compound is 763 Å^3/C_{60}, which is comparable to Rb_2CsC_{60} ($T_c = 31$ K). However, no superconductivity was observed above 2 K at ambient conditions. Later on, an ac-susceptibility measurement showed that superconductivity of $T_c = 28$ K recovers above 10 kbar [7]. These properties suggest that $NH_3K_3C_{60}$ is on the verge of the superconductor–nonsuperconductor boundary.

New synthesis routes using NH_3 produced several other materials which retain the $(C_{60})^{-3}$ state but do not superconduct at ambient temperature [7, 8]. These results suggest that ammoniation is a useful technique to form a new subfamily of fullerides, and that study of alkali ammonia complex fullerides might help in constructing a unified picture of criteria for metallic nature and superconductivity in fullerides. Here we report two properties of alkali ammonia complex fullerides. First, we describe our recent success in the synthesis of new superconducting fullerides, including ammonia. The new compounds do not follow the conventional relation between T_c and lattice parameters. Secondly, we report that $NH_3K_3C_{60}$ undergoes a metal–insulator transition which destroys

*Present address: The University of Carolina at Chapel Hill, Department of Physics and Astronomy, Chapel Hill, NC 27599, USA.

†Present address: Department of Chemical Physics, University of Groningen, Nijenborgh 4, The Netherlands.

the superconductivity expected from the empirical relation. On the basis of the experimental results, we discuss the structural criteria for the metallic state and superconductivity.

2. SUPERCONDUCTIVITY OF $(NH_3)_xNAA_2C_{60}$

Success in the growth of Cs_3C_{60} suggests that synthesis in liquid ammonia is a promising method in the search for new fullerides [8]. Here we describe the synthesis and structure of $(NH_3)_xNaA_2C_{60}$ (A = K and Rb). The combination of one small Na ion and two large K or Rb ions has been known to be unstable without NH_3. Since there are one large octahedral and two small tetrahedral interstitial sites per C_{60}, the above combination is excluded due to the selectivity of the interstitial sites [9]. Reaction took place in liquid ammonia which was condensed in a glass tube through a stainless-steel tube and kept at about 200 K in a dry ice/acetone slush. After both alkali metals and C_{60} powders have dissolved in the liquid ammonia, the ammonia was slowly vaporized. Thus obtained powders contain a considerable amount of solvent (about one NH_3 molecule per C_{60}). To control the ammonia content, we dried the sample at 120°C and 190°C under dynamic vacuum. The ammonia content decreases on increasing this temperature down to $x \sim 0.5$. Heating the samples above 200°C resulted in a phase separation, indicating that NaA_2C_{60} is unstable without NH_3. Here the ammonia content was estimated by the relative intensity ratio of ^1H and ^{13}C NMR.

Fig. 1 shows Cu Kα X-ray diffraction patterns for three samples of $(NH_3)_xNaK_2C_{60}$, which are named KA, KB, and KC. All the patterns are indexed as single phases of fcc. This result is in sharp contrast with that for K_3C_{60}, where deformation to an orthorhombic structure occurred in the monoammoniated compound. Especially in the case of the sample KC, which turned out to have the chemical composition $NH_3NaK_2C_{60}$, the chemical difference from $NH_3K_3C_{60}$ is that one potassium is substituted by one sodium. Thus one can understand that the reason for the fcc structure in $(NH_3)_xNaK_2C_{60}$ is related to the small size of Na ions compared to K ions. A notable feature of fcc $(NH_3)_xNaK_2C_{60}$ is that the lattice parameter is controlled from 14.35 Å to 14.40 Å by the ammonia concentration x. Fig. 1 shows the fcc lattice parameter and ammonia composition x estimated by the Rietveld refinements. The x values determined by NMR and the refinement of diffractograms are qualitatively consistent.

The lattice parameter increases with increasing ammonia concentration. The same features are observed in $(NH_3)_xNaRb_2C_{60}$, where the lattic parameter varies from 14.50 to 14.53 Å.

We performed the structural analysis of $(NH_3)_xNaK_2C_{60}$ and $(NH_3)_xNaRb_2C_{60}$, both of which

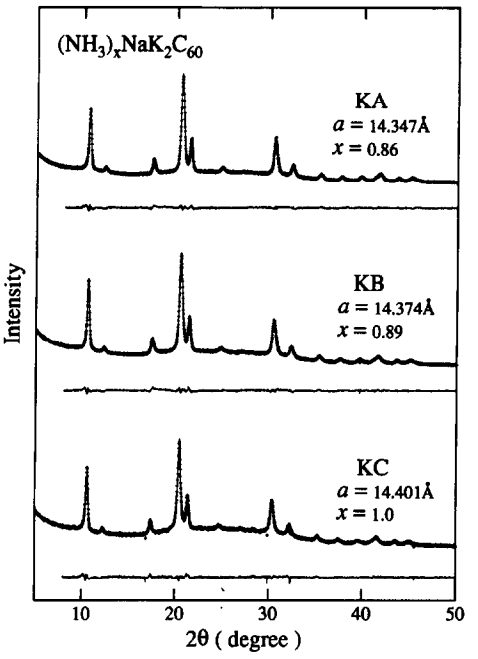

Fig. 1. X-ray diffractogram of three samples of $(NH_3)_xNaK_2C_{60}$. Crosses show experimental data collected with Cu K $\propto$ radiation with a rotating anode source. The solid lines are Rietveld fits to the model described in the text, with the differences shown on the same scale beneath the experimental and calculated patterns.

have essentially the same structure. The intensity profile of the diffraction pattern of $(NH_3)_xNaK_2C_{60}$ is similar to that of $(NH_3)_4Na_2CsC_{60}$, in which the octahedral interstitial site is occupied by a tetrahedron of four NH_3 molecules with Na at the centre, and the remaining Na and Cs occupy the tetrahedral site [4]. In particular, the relative intensity of the (111) peak, which is located at about $2\Theta \sim 10.5°$, is stronger in $(NH_3)_xNaK_2C_{60}$ than in K_3C_{60}. This means that there is a light element in the octahedral site. Thus, we modelled that Na and NH_3 occupy the octahedral site and K occupies the tetrahedral sites. In fact, a preliminary intensity simulation, using the LAZY-PULVERIX program (K. Yvon, W. Jeitschko and E. Parthe) where Na and K ions occupy the octahedral and tetrahedral sites, respectively, gives a reasonable agreement with the experimental data, assuming the Na occupancy is 1.9. Since the electron counts of Na^+ and NH_3 are the same, this simulation supports our model in which almost one Na^+ ion and one NH_3 molecule occupy the octahedral site.

Reitveld refinement was performed by the RIETAN program (F. Izumi) in space group $Fm\bar{3}m$. In this refinement, we replace NH_3 molecules by Ne atoms which have the same electron counts. We started a model with the ammonia content x = 1, where all K ions occupy the tetrahedral site and the Na and NH_3 occupy the octahedral site (Fig. 2(a)). The Ne atom was placed at the 32(f)(x,x,x) positions on the corner of the cubes. Since, in the monoammoniated K_3C_{60} the

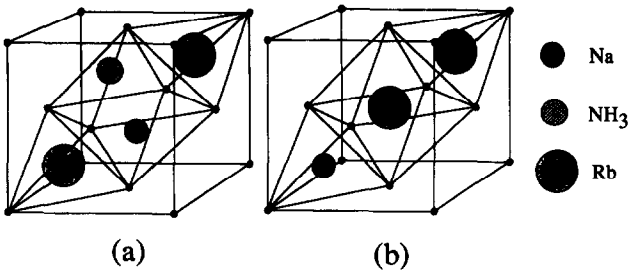

Fig. 2. Schematic representation of the structural model of $(NH_3)_xNaA_2C_{60}$ (A = K and Rb). Small dots show C_{60} molecules and the ammonia molecules are expressed by a sphere. In the configuration (a), the Na–NH_3 clusters in the octahedral site are randomly aligned along the eight equivalent (111) orientations. The whole crystal is regarded as a solid solution of the two configurations.

octahedral potassium ion is off-centred, we allowed the Na ion to be off-centred [6] and placed at the 32(f)(y,y,y) positions. In other words, the Na-NH_3 cluster along the body diagonal of the cube occupies the eight equivalent disordered orientations.

Since the NMR measurement tells us that the ammonia composition x is smaller than 1, the above model should be modified and the x value should be refined. We assumed that in the NH_3-deficient site, the remaining Na ions are replaced by heavy elements (K and Rb) (Fig. 2(b)). This model is based on the experimental result that the relative intensity of the (111) peak decreases, as the ammonia composition decreases (C → B → A). This trend is more clearly observed in $(NH_3)_xNaRb_2C_{60}$. Therefore, the whole crystal is regarded as a microscopic mixture of the following two configurations (Fig. 2). The octahedral site is occupied by NH_3 and Na with the probability x, while the tetrahedral site is occupied by K(Rb) ions (Fig. 2(a)). The remaining octahedral site is occupied by K ions with the probability $1 - x$, with the tetrahedral site occupied by K(Rb) and Na (Fig. 2(b)).

Carbon positions were allowed to vary only radially to preserve the shape of the C_{60} molecule. The orientation of C_{60} molecules was assumed to be merohedrally disordered as in the case of K_3C_{60} [10]. We found that the x value and the position of Na^+ and Ne are strongly correlated. Thus we first fixed the Na–Ne (octahedral) distance at 2.5 Å, which is a typical distance of between an Na ion and the N atom of ammonia [4]. Then we removed the constraint of Na–Ne distance and refined the Na and Ne positions with fixed x. The refinement converged rapidly to the results shown in Fig. 1. The results for the sample C is tabulated in Table 1. Only in this case, the refinement was successful when we fixed the ammonia composition as $x = 1$.

The ammonia content x estimated by NMR and Rietveld refinement shows the same trend, decreasing with the drying temperature. Na ions are shifted from the octahedral centre by 0.5–0.6 Å. Fig. 3 shows the R_{wp}-factors as a function of the position of the octahedral Na for the sample $(NH_3)_xNaRb_2C_{60}$ ($x = 0.60$ as determined by NMR), and reveal that the R-factors show a sharp minimum when the Na ion is shifted by 0.50 Å from the octahedral centre. The position of Na^+ shows a systematic trend: the distance between Na^+ and the octahedral centre is smaller with decreasing x. Although the shift of cations from the centre of the octahedral site is suggested by several experiments such as NMR [11] and EXAFS [12] measurements, no XRD evidence has ever been reported. For instance, according to Zhou and Cox, the refinement of the XRD pattern of Rb_3C_{60} was not improved by shifting alkali metals from the centre of the inerstices [13]. These result indicate that in the conventional A_3C_{60}-type superconductors, the shift of the octahedral cation is not detectable even if it may not be zero. The displacement of 0.5–0.6 Å of the octahedral Na is considerably smaller than that of the octahedral K in $NH_3K_3C_{60}$ (1.42 Å)[6]. The small shift might be a part of the reason for the preserved cubic structure in $(NH_3)_xNaK_2C_{60}$ and $(NH_3)_xNaRb_2C_{60}$, without structural distortions as seen in $NH_3K_3C_{60}$. The results of the Rietveld analysis confirm that the new compounds are examples of the fcc superconductors with the off-centred alkali ions in the octahedral sites.

Table 1. Atomic coordinates, fractional site occupancies N, and thermal factors B, for the sample KC. The refinement was carried out with the chemical formula $NH_3NaK_2C_{60}$, assuming the space group $Fm\bar{3}m$ and $a = 14.401$ Å. NH_3 molecules are replaced by Ne atoms

	Site	x	y	z	N	B/Å^2
C1	96*j*	0.0	0.0501	0.2431	0.5	0.9
C2	192*i*	0.2122	0.0811	0.1001	0.5	0.9
C3	192*i*	0.1812	0.1621	0.0502	0.5	0.9
Na	32*f*	0.4761	0.4761	0.4761	0.125	5.0
Ne	32*f*	0.5810	0.5810	0.5810	0.125	5.0
K	8*c*	0.25	0.25	0.25	1.0	6.5

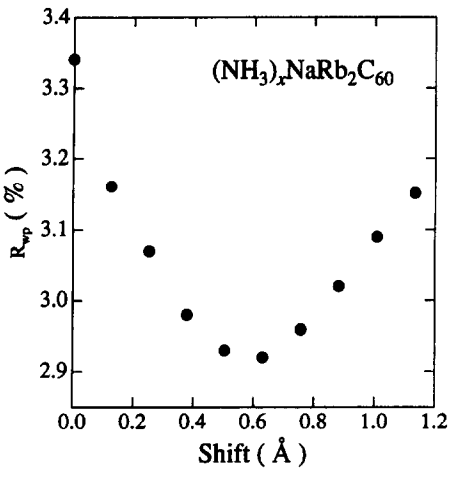

Fig. 3. R_{wp} value as a function of the position of octahedral sodium measured from the centre of the interstitial site for $(NH_3)_xNaRb_2C_{60}$ with $x = 0.82$.

Fig. 4 shows temperature dependence of magnetization for three samples of $(NH_3)_xNaK_2C_{60}$, which was taken at 10 Oe under a zero-field-cooled condition. Bulk superconductivity is unambiguously confirmed by the large shielding fraction ~100%. It is noted that T_c changes with ammonia concentration. The relation between T_c and cell volume V per C_{60} is shown in Fig. 5. Surprisingly, T_c decreases with increasing cell volume, in remarkable contrast with the conventional superconducting fullerides [2, 14]. Another interesting implication of $(NH_3)_xNaK_2C_{60}$ and $(NH_3)_xNaRb_2C_{60}$ is that the T_c is suppressed in spite of the fcc structure of these compounds. A decrease in T_c indicates that a negative factor exists for the superconductivity even in fcc structures.

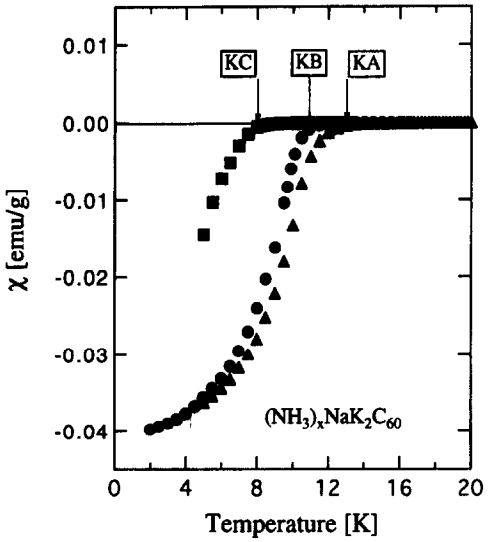

Fig. 4. Temperature dependence of magnetic susceptibility for $(NH_3)_xNaK_2C_{60}$ with different ammonia concentration. Data were collected at 10 Oe after a zero-field cooling. The labels KA, KB, KC correspond to those in Fig. 1.

Here we discuss the effect of ammonia on T_c. Inclusion of ammonia may significantly affect the structure and electronic properties. Nonetheless, a fact that the plot for $(NH_3)_4Na_2CsC_{60}$ falls on the conventional line strongly suggests that the ammoniation itself does not affect superconductivity. In fact, preliminary Raman spectra of the pentagonal pinch mode with A_g symmetry show that the molecular value remains at $(C_{60})^{-3}$ within the experimental error both for $(NH_3)_xNaK_2C_{60}$ and $(NH_3)_xNaRb_2C_{60}$. In other ammoniated materials, there is no evidence for the deviation of valence from the $(C_{60})^{-3}$ state. These results indicate that the neutral ammonia molecules do not affect the valence of C_{60}. Fig. 5 shows that there are three groups of low-T_c materials. They are $NH_3K_3C_{60}$, $(NH_3)_xNaK_2C_{60}$ and $(NH_3)_xNaRb_2C_{60}$. All of them contain one or less ammonia molecule per C_{60} in the octahedral site, and as a result, cations are displaced from the centre of the octahedral site by ammonia molecules. These results suggest that the shift of octahedral cations from the centre position is a dominant factor in the suppression of superconductivity.

One should consider the effect of disorder since new kinds of disorder are introduced in $(NH_3)_xNaA_2C_{60}$ due to the off-centred cations. However, it is also noted that superconductivity of conventional fullerides is not affected by several kinds of disorder, such as rotational disorder and substitutional disorder of the interstitial sites. Suppression of T_c only in the systems containing off-centred cations indicates that the position of the cations plays a crucial role in the superconductivity of fullerides.

Recent experiments by Yildirim et al.[15] show that T_c has a sharp maximum at the $(C_{60})^{3-}$ state. Combining their and our experiments, we conclude that the on-centred cation and the half-filled state of the t_{1u} band is crucial for the high T_c of fullerene superconductivity. These experimental results remind us of the exotic pairing mechanisms of Chakravarty et al. [16], Varma et al. [17], and others. These are based on the dynamical charge disproportionation $2(C_{60})^{3-} \rightarrow (C_{60})^{2-} + (C_{60})^{-4}$ in the real space image. The disproportionation might occur in the presence of "negative U", caused by changing the intramolecular bonding characters [16] or deformation of the molecular skeleton [17]. The latter type of energy gain is enhanced in the existence of Jahn–Teller-type electron-molecular vibration interactions. K-space condensation into $(C_{60})^{2-}$ and $(C_{60})^{4-}$ states produces superconductivity.

About 0.6 Å displacement of alkali ion from the centre of the octahedral site makes the local potential on the C_{60} anion non-cubic. The non-cubic local Coulomb potential on C_{60} from the surrounding alkali ions results in a static rather than dynamic charge disproportionation. Due to the static deformation, pairing is significantly

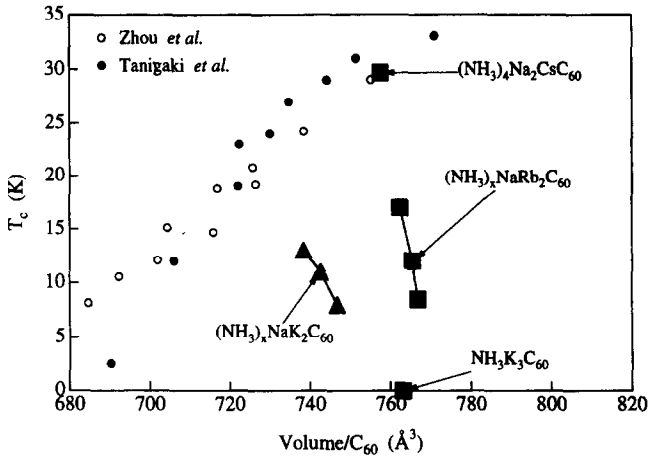

Fig. 5. Relation between T_c and the volume V per C_{60} for alkali–ammonia complex fullerides. Small open and filled dots represent conventional A_3C_{60} superconductors from Zhou et al. [2] and Tanigaki et al. [14], respectively.

suppressed, being qualitatively consistent with the low T_c in the compounds containing the off-centred cations.

3. METAL–INSULATOR TRANSITION IN $NH_3K_3C_{60}$

As to the position of octahedral cations, $NH_3K_3C_{60}$ is the extreme case, because of two reasons. Firstly, the shift of octahedral potassium is much larger than that of sodium in $(NH_3)_xNaA_2C_{60}$, and the secondly, the superconductivity is completely destroyed in $NH_3K_3C_{60}$. In this sense, $NH_3K_3C_{60}$ is a unique compound. We performed electron spin resonance (ESR), magnetic susceptibility, and ^{13}C-nuclear magnetic resonance (NMR) measurements at ambient pressure to clarify the reason for the absence of superconductivity and the low-temperature electronic states [18].

$NH_3K_3C_{60}$ was prepared by exposing NH_3 gas to preformed K_3C_{60} [6, 7]. The starting K_3C_{60} was synthesized by a direct reaction of K-vapour and C_{60} powders and a following one-month anneal at 400°C. The thus obtained single phase K_3C_{60} powders (20–50 mg) were loaded in a glass tube (5 mm in diameter), evacuated to 10^{-3} torr and exposed to dry ammonia at room temperature and 0.5 atm for 20 minutes. After the reaction, the glass tube was sealed under 0.5 atm NH_3. The samples were annealed at 100°C for another month. Sample characterization was made by means of X-ray diffraction and NMR. The former clearly showed the phase purity and the latter confirmed that the ammonia concentration is $x \sim 1$.

9-GHz ESR data were collected on typically 2–5 mg samples loaded in quartz tubes, using a JEOL JES-RE3X apparatus. The spin susceptibility was estimated from the areas of the ESR signal, which were calibrated by a standard tetramethylpiperidinooxy sample. K_3C_{60} shows a single Lorentzian ESR signal at room temperature. The spin susceptibility at room temperature determined by the ESR was 4.3×10^{-4} emu/mole for K_3C_{60}, which is smaller than the reported values [19, 20]. The g-value ($g = 2.004$), and the peak-to-peak linewidth ($\delta H = 1.4$ mT) are consistent with the literature [20].

The ESR signal at room temperature is shown in Fig. 6 for K_3C_{60} and $NH_3K_3C_{60}$. The line shape and peak position of $NH_3K_3C_{60}$ are very similar to those of K_3C_{60} at room temperature. The relative integrated intensity for $NH_3K_3C_{60}$ was carefully measured using several samples. This experiment leads us to a conclusion that the intensity of $NH_3K_3C_{60}$ is the same as that of K_3C_{60} within experimental error at room temperature.

At low temperatures, we observed different behaviours in $NH_3K_3C_{60}$ and K_3C_{60}. Fig. 7 shows the temperature dependence of integrated intensities for $NH_3K_3C_{60}$ and K_3C_{60}. The intensity is normalized by the room temperature value of K_3C_{60}. The intensity for $NH_3K_3C_{60}$ increases with decreasing temperature, while it shows a slight decrease for K_3C_{60}. In

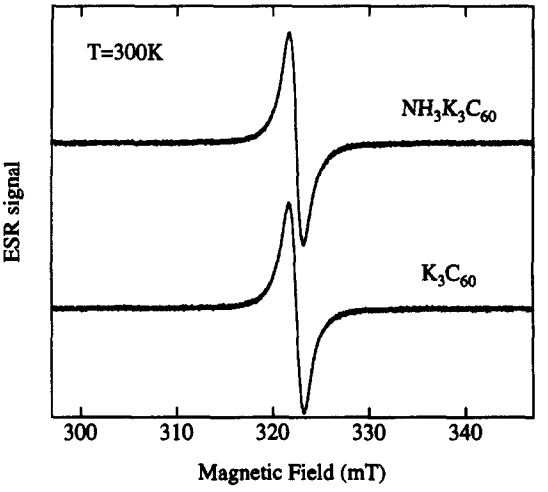

Fig. 6. Room temperature ESR signals for $NH_3K_3C_{60}$ and K_3C_{60} collected at ~9 GHz.

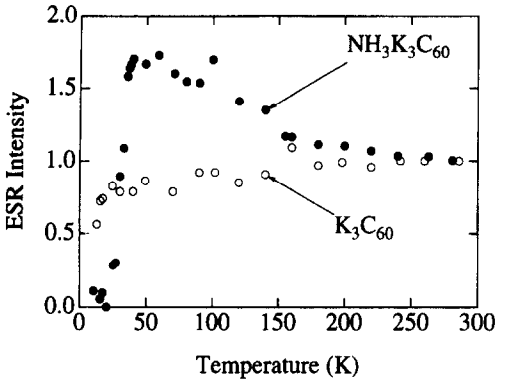

Fig. 7. Intergrated ESR intensity for $NH_3K_3C_{60}$ and K_3C_{60} as a function of temperature. The intensities are normalized by the room temperature value of K_3C_{60}.

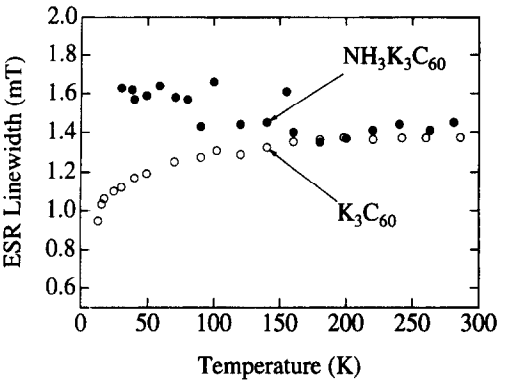

Fig. 8. Temperature dependence of the ESR linewidth for $NH_3K_3C_{60}$ and K_3C_{60}.

$NH_3K_3C_{60}$, a sharp impurity line (~0.1 mT in width) appears below 150 K, in addition to the intrinsic broad line (δH~1.5 mT), as shown in the inset of Fig. 9. The integrated intensity of the sharp line approximately follows the Curie law with about 2% localized spins per C_{60} molecule. Fig. 7 shows the contribution of only the broad intrinsic line. The ESR signal of $NH_3K_3C_{60}$ suddenly decreases at 40 K, and eventually disappears leaving the narrow impurity line below 20 K.

The increase in the ESR intensity upon cooling is in sharp contrast to the behaviour of A_3C_{60}, typically shown in Fig. 7 for K_3C_{60}. The slight decrease in the intensity of K_3C_{60} is explained by the reduction of $N(\epsilon_F)$ due to the lattice contraction [20]. The increase in the ESR intensity upon cooling observed in $NH_3K_3C_{60}$ is rather exceptional for conventional A_3C_{60} compounds, indicating that the electronic structures are significantly modified by intercalation of ammonia. From ESR data alone, we cannot tell whether $NH_3K_3C_{60}$ is metallic or not. However, taking account of the susceptibility and NMR data shown below, we conclude that the high temperature state is metallic. The drop in ESR intensity at 40 K strongly suggests the occurrence of a metal–insulator transition.

Fig. 8 shows the temperature dependence of peak-to-peak linewidths for $NH_3K_3C_{60}$ and K_3C_{60}. The ESR linewidth slightly decreases with temperature in K_3C_{60}, whereas the width is almost constant in $NH_3K_3C_{60}$. The temperature dependence of the ESR linewidth is a useful means to investigate the metallic state of alkali-intercalated C_{60} materials [20]. The observed temperature dependence in $NH_3K_3C_{60}$ is very similar to that of A_3C_{60} materials with large lattice parameters and with high T_c, such as Rb_3C_{60} [21, 20]. This result indicates that $NH_3K_3C_{60}$ is a narrow band metal.

Below 40 K, the intrinsic broad signal suddenly disappears leaving the sharp impurity component, indicating the occurrence of a metal–insulator transition. The temperature variation of the linewidth below T_c is an important clue for identifying the low temperature electronic states. The impurity line, however, makes the estimation of linewidths extremely difficult. As an indirect probe of the linewidth, we plot in Fig. 9 the temperature dependence of the ESR signal at about 15 mT lower field than the resonance position. Since the linewidth of the impurity line is about 0.1 mT, there is no effect of impurity at this magnetic field. At the metal–insulator transition temperature, T_{MI}, no signal is observed because the intrinsic linewidth is narrow enough (~1.6 mT). As temperature is reduced, the ESR signal comes out forming a peak at about 25 K. This peak indicates that upon cooling through 40 K, the intrinsic linewidth first increases and then the signal intensity decreases. In other words, the ESR signal disappears with the line broadening below 40 K. The broadening of the linewidth is strong evidence of the antiferromagnetic state of the low temperature phase.

Fig. 10 shows the magnetic susceptibility of $NH_3K_3C_{60}$ and K_3C_{60}. The raw data involved the Curie tail at low temperature, which is approximated by the formula $1.0\times10^{-2}/(T + \Theta)$ (emu/mole), which corresponds to 2.6% spins per C_{60} (here, Θ = 1 K). The concentration of the impurity spins agrees with the ESR data. In Fig. 2, the Curie part was subtracted from the raw data. The diamagnetic contribution from C_{60}, potassium ion, and ammonia was not subtracted. The susceptibility at room temperature is 5.0×10^{-4} amu/mole. This value is close to that for K_3C_{60} ($4.7–5.9\times10^{-4}$) emu/mole after Ramirez et al. [22]. Susceptibility at room temperature does not change very much upon ammoniation, in fair agrement with the ESR results. The susceptibility increases with decreasing temperature, also consistent with the ESR intensity. The susceptibility value at low temperature reaches 1×10^{-3} emu/mole, which is comparable to the raw data for Rb_3C_{60} [22]. Similar behaviour of the metallic state is often observed in strongly correlated electron systems such as transition metal oxides. $NH_3K_3C_{60}$ can be viewed as a correlated metal.

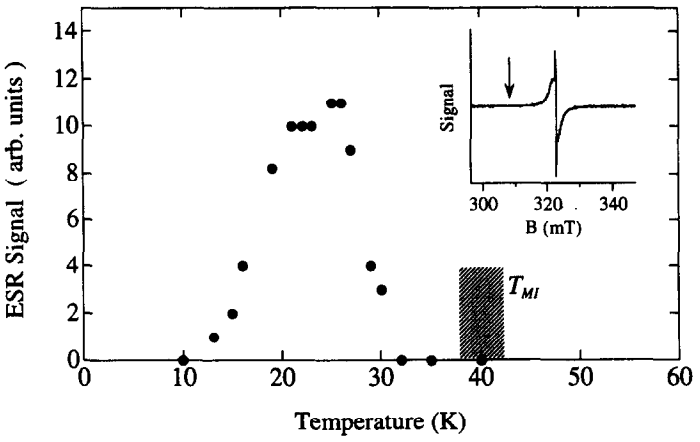

Fig. 9. Temperature dependence of the ESR signal at a magnetic field 15 mT lower than the resonance field indicated by arrows in the inset.

In marked contrast with the ESR, the susceptibility does not show any remarkable anomaly around 40–45 K, being almost constant below 50 K. The non-vanishing susceptibility at the lowest temperature implies that the magnetic excitations remain in the low temperature state. Hence, a possible explanation for the contrasting behaviours in the ESR intensity and susceptibility might be an antiferromagntic transition. In the low temperature phase, the charge is localized and the spin is ordered antiferromagnetically.

For a further investigation of the metal–insulator transition and the low temperature state, we measured ^{13}C-NMR for $NH_3K_3C_{60}$ at 40.6 MHz. The ^{13}C spin-lattice relaxation time T_1 was determined by a conventional saturation recovery method. The ^{13}C-NMR spectra were obtained by a pulse Fourier transformation [23]. The peak position was measured as a shift from that of trimethylsilane standard. The ^{13}C-NMR spectra of $NH_3K_3C_{60}$ has a sharp single peak with a shift of 195 ± 2 ppm at room temperature. This shift is slightly larger than that of K_3C_{60} (187 ± 2 ppm). The sharp NMR spectra (13 ppm in width) indicate that C_{60} molecules rotate at room temperature. The signal becomes broader below 150 K, implying the freezing of molecular rotation.

Fig. 11 shows the T_1^{-1} against temperature below 100 K. Above 40 K, the data approximately fall in a relation $1/T_1 = AT + B$. Assuming that the B-term (=0.2 s^{-1}) is attributed to the paramegnetic impurities, the concentration of impurities is roughly estimated to be 3%, which is not far from the observed paramagnetic impurities in magnetic susceptibility and ESR. Since the NMR relaxation rate $1/T_1$ is the sum of contributions from the paramagnetic impurities and intrinsic spins, the first term of the above relation corresponds to the Korringa law. The A-value is derived to be 0.0124 $K^{-1}s^{-1}$ and 0.0061 $K^{-1}s^{-1}$ for $NH_3K_3C_{60}$ and K_3C_{60}, respectively. Corresponding lines are drawn in Fig. 11. Since $A \propto N(\epsilon_F)^2$, the apparent $N(\epsilon_F)$ for $NH_3K_3C_{60}$ is about 1.4 times larger than that for K_3C_{60}. Considering that the spin susceptibility is proportional to the apparent

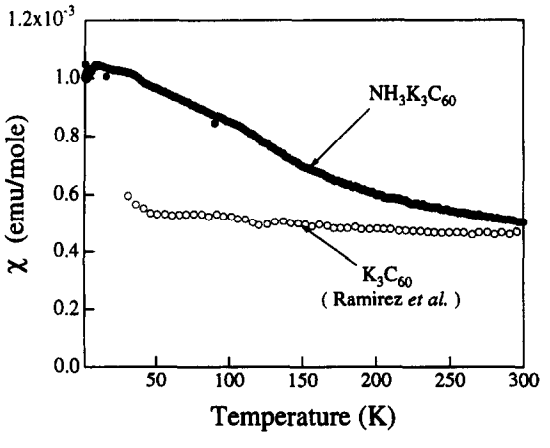

Fig. 10. Magnetic susceptibility of $NH_3K_3C_{60}$ and K_3C_{60}. The Curie tail attributable to impurities are subtracted from the raw data. The data for K_3C_{60} was taken from Ramirez et al. [22].

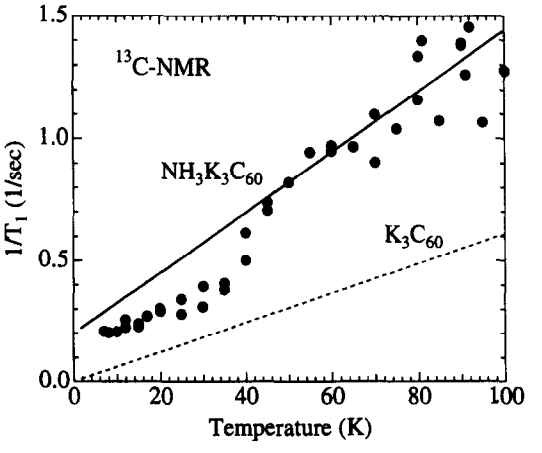

Fig. 11. Temperature dependence of T_1^{-1} for ^{13}C-NMR for $NH_3K_3C_{60}$. Filled circles show the experimental data and the solid straight line is a fit to the relation $1/T_1 = AT + B$ (see text). The dashed line shows an approximation of the T_1^{-1} for K_3C_{60}.

$N(\epsilon_F)$, the enhancement of the A-value in $NH_3K_3C_{60}$ qualitatively agrees with the data of the ESR and magntic susceptibility. Here, we note that the above discussion is very preliminary because the relation $1/T_1 = AT + B$ is valid when the susceptibility is temperature-independent, while in reality the susceptibility is temperature-dependent even below 100 K.

Another notable feature is the deviation from the Korringa relation observed at 40 K, corroborating the occurrence of the metal–insulator transition. Anomalies at 40 K in ESR and NMR provide convincing evidence for an insulating low-temperature state in $NH_3K_3C_{60}$.

As to the nature of the low temperature phase, we did not observe any enhancement of T_1^{-1} which is frequently found at the antiferromagnetic or spin density wave transition in organic conductors [24]. If an internal field is switched on due to the magnetic ordering, the linewidth should be broadened. However, the line shape does not change very much at the transition temperature. These results imply that the magnetic moment is smaller than the detection limit.

A possible explanation for the ESR, susceptibility, and NMR data is an antiferromagnetic insulating state with an extremely small magnetic moment. In fact, the magnetic moment can be very small in molecular conductors. For example, a zero-field muon spin relaxation experiment clarified an SDW state with a magnetic moment of $\sim 3\text{x}10^{-3}\mu_B$ in $(BEDT\text{–}TTF)_2KHg(SCN)_4$ [25]. Such a small moment cannot be detected by a standard NMR technique.

4. SUMMARY

We have shown that alkali ammonia complex fullerides form a new group of materials with the valence state of $(C_{60})^{3-}$ having large lattice parameters.

$NH_3K_3C_{60}$ involves one ammonia molecule per C_{60} in the octahedral site. The shift of the octahedral potassium ion from the centre is significantly large ($\sim$1.4 Å) and the unit cell is distorted into faced-centred orthorhombic. In this compound, superconductivity is completely suppressed and the ground state is insulating, as was confirmed by ESR and NMR measurements.

The occurrence of a metal–insulator transition and the absence of superconductivity at ambient pressure is a fundamental question to be solved. The unit cell volume V is almost identical to that of fcc Rb_2CsC_{60} with T_c = 31 K. The symmetry reduction to orthorhombic structure might be part of the reason for the disappearance of superconductivity. But this is not fatal for superconductivity, because $NH_3K_3C_{60}$ does superconduct under high pressure in the orthorhombic structure [7]. Considering the case of $(NH_3)_xNaA_2C_{60}$, the dominant factor for suppressing superconductivity are the off-centred octahedral cations. The non-cubic local field due to the shift of cations makes conduction elctrons localized. Even in the metallic state, the electron correlation effect is clearly seen in the spin susceptibility. In the low temperature insulating state, evidence for the antiferromagnetic state was found in the ESR spectra.

In conclusion, alkali ammonia complex fullerides form a novel group of materials that exhibits unusual properties. These multinary systems are valuable for a full understanding of the superconductivity of fullerides.

Acknowledgements—The authors are grateful to K. Tanigaki, M. Kosaka, D. Sugiura, T. Furudate and H. Hayashi for discussion and experimental help. This work was supported by a Grand-in-Aid from the Ministry of Education, Sports, Science and Culture, Japan Society for Promotion of Science, and Yamada Science Foundation.

REFERENCES

1. Fleming, R.M., Ramirez, A.P., Rosseinsky, M.J., Murphy, D.W., Haddon, R.C., Zahurak, S.M. and Makhija, A.V., *Nature (London)*, 1991, **352**, 787.
2. Zhou, O., Vaughan, G.B.M., Zhu, Q., Fischer, J.E., Heiney, P.A., Coustel, N., McCauley, J.P. Jr and Smith III, A.B., *Science*, 1992, **255**, 833.
3. Ramirez, A.P., *Superconductivity Review*, 1994, **1**, 1.
4. Zhou, O., Fleming, R.M., Murphy, D.W., Rosseinsky, M.J., Ramirez, A.P., van Dover, R.B. and Haddon, R.C., *Nature (London)*, 1993, **362**, 433.
5. Ishiguro, T. and Jamaji, K., *Organic Superconductors*. Springer-Verlag, 1990.
6. Rosseinsky, M.J., Murphy, D.W., Fleming, R.M. and Zhou, O., *Nature (London)*, 1993, **364**, 426.
7. Zhou, O., Palstra, T.T.M., Iwasa, Y., Fleming, R.M., Hebard, A.F., Sulewski, P.E., Murphy, D.W. and Zegarski, B.R., *Phys. Rev.*, 1995, **B52**, 483.
8. Palstra, T.T.M., Zhou, O., Iwasa, Y., Sulewski, P.E., Fleming, R.M. and Zegarski, B.R., *Solid State Commun.*, 1995, **93**, 327.
9. Shimoda, H., Iwasa, Y., Miyamoto, Y., Maniwa, Y. and Mitani, T., *Phys. Rev.*, 1996, **B54**, R15653.
10. Stephens, P.W., Mihaly, L., Lee, P.L., Whetton, R.L., Huang, S.-M., Kaner, R., Diederich, F. and Holczer, K., *Nature (London)*, 1991, **351**, 632.
11. Walstedt, R.E., Murpy, D.W. and Rosseinsky, M.J., *Nature (London)*, 1993, **362**, 611.
12. Hiroswa, H., Kimura, H., Mizuki, J. and Tanigaki, J., *Phys. Rev.*, 1995, **B51**, 3038.
13. Zhou, O. and Cox, D.E., *J. Phys. Chem. Solids*, 1992, **53**, 1373.
14. Tanigaki, K., Hirosawa, I., Ebbesen, T.W., Mizuki, J., Shimakawa, Y., Kubo, Y., Tsai, J.S. and Kurosawa, S., *Nature (London)*, 1992, **356**, 419.
15. Yildirim, T., Barbedette, L., Fischer, J. E., Lin, C. L., Robert, J., Petit, P. and Palstra, T. T. M., *Phys. Rev. Lett.*, 1996, **77**, 167.
16. Chakravarty, S., Kivelson, S.A., Salkola, M.I. and Tewari, S., *Science*, 1991, **254**, 989.
17. Varma, C.M., Zaanen, J. and Raghavachari, K., *Science*, 1991, **254**, 989.
18. Iwasa, Y., Shimoda, H., Palstra, T.T.M., Maniwa, Y., Zhou, O. and Mitani, T., *Phy. Rev.*, 1996, **B53**, R8836.
19. Wong, W.H., Hanson, M.E., Clark, W.G., Grüner, G., Thompson, J.D., Whetten, R.L., Huang, S.-M., Kaner, R.B., Diederich, F., Petit, P., André, J.-J. and Holczer, K., *Europhys. Lett.*, 1992, **18**, 79.
20. Tanigaki, K., Kosaka, M., Manako, T., Kubo, Y., Hiroswa, I., Uchida, K. and Prassides, K., *Chem. Phys. Lett.*, 1995,

240, 627.Tanigaki, K., Hirosawa, I. and Prassides, K., in *Physics and Chemistry of Fullerenes and Derivertives*, ed. H. Kuzmany, J. Fink, M. Mehring and S. Roth. World Scientific, Singapore, 1995, p.385.
21. Jánosy, A., Chauvet, O., Pekker, S., Cooper, J.R. and Forro, L., *Phys. Rev. Lett.*, 1993, **71**, 1091.
22. Ramirez, A.P., Rosseinsky, M.J., Murphy, D.W. and Haddon, R.C., *Phys. Rev. Lett.*, 1992, **69**, 1687.
23. Maniwa, Y., Saito, T., Ohi, A., Mizoguchi, K., Kume, K., Kikuchi, K., Ikemoto, I., Suzuki, S., Achiba, Y., Kosaka, M., Tanigaki, K. and Ebbesen, T.W., *J. Phys. Soc. Jpn.*, 1994, **63**, 1139.
24. Jérome, D., in *Organic Conductors: Fundamentals and Applications*, ed. J.-P. Farges. Marcel Dekker, Inc., New York, 1994, p.405.
25. Pratt, F.L., Sasaki, T., Toyota, N. and Nagamine, K., *Phys. Rev. Lett.*, 1995, **74**, 3892.